Radiological Physics and Technology (2019) 12:357–361
https://doi.org/10.1007/s12194-019-00528-4

Delineation of the intratemporal facial nerve in a cadaveric specimen on diffusion tensor imaging using a 9.4 T magnetic resonance imaging scanner: a technical note

Daniel Thomas Ginat[1] · John Collins[1] · Florian Christov[2] · Erik G. Nelson[2] · Michael B. Gluth[2]

Received: 17 April 2019 / Revised: 23 July 2019 / Accepted: 24 July 2019 / Published online: 29 July 2019

Abstract
The purpose of this study was to determine whether the intratemporal facial nerve could be delineated on 9.4 T magnetic resonance imaging (MRI) using T2-weighted and diffusion tensor imaging (DTI). DTI using a *b* value of 3000 and an isotropic resolution of 0.4 mm^3 on a 9.4 T MRI scanner was performed on a whole-block celloidin-embedded cadaveric temporal bone specimen of a 1-year-old infant with normal temporal bones. The labyrinthine, tympanic, and mastoid segments of the facial nerve and the chorda tympani nerve were readily depicted on DTI. Therefore, DTI performed using a high *b* value on a high-field strength MRI scanner could help evaluate the intratemporal facial nerve in whole temporal bone ex vivo specimens.

Keywords 9.4 T MRI · Facial nerve · Temporal bone · DTI · In vitro

Abbreviations

DTI	Diffusion tensor imaging
MRI	Magnetic resonance imaging
CT	Computed tomography
TR	Repetition time
TE	Echo time

1 Introduction

Ultra-high-field 9.4 T and 11.7 T magnetic resonance imaging (MRI) scanners can provide excellent-resolution images of ex vivo specimens of the temporal bone [1–3]. The structures that can be appreciated via ultra-high-resolution MRI include the osseous spiral lamina, Reissner's membrane, the membranous spiral lamina, and the spiral ligament within the cochlea [1–3]. The acquisition and processing of temporal bone specimens for a histopathological study are a time-consuming process that takes approximately 1 year, and such specimens are a rare commodity. After a standardized process of decalcification, followed by embedding in celloidin, these specimens are typically cut in a single plane to be mounted on slides for a microscopic study. After this process is performed, some of the 3-dimensional (3D) orientations can be difficult to appreciate. Furthermore, delicate tissues are commonly damaged during this process.

Although micro-computed tomography (CT) can provide excellent anatomical delineation of bony structures in the temporal bone [4, 5], it does not readily depict the details of soft-tissue structures, such as the nerves. However, ultra-high-field MRI could acquire archived images, allowing a detailed assessment of nerve structures in multiple planes, which might augment standard histological preparation schemes. This may be particularly useful in specimens with rare disease entities or with developmental malformations in the temporal bone [1–3].

MR diffusion tensor imaging (DTI) is effective in identifying the position of the facial nerve in patients with cerebellopontine angle (CPA) tumors, which optimizes tumor excision while preserving neurological integrity [6–10]. However, anatomic delineation of middle ear structures, including the facial nerve, on MRI in the clinical setting remains limited [10]. The intricate course of the facial nerve through the temporal bone is relevant in otologic surgeries, as it often traverses the surgical field [11]. The goal of this study was to determine the extent to which the intratemporal

✉ Daniel Thomas Ginat
dtg1@uchicago.edu

[1] Department of Radiology, University of Chicago, Pritzker School of Medicine, 5841 S Maryland Avenue, Chicago, IL, USA

[2] Department of Surgery, Section of Otolaryngology, University of Chicago, Pritzker School of Medicine, Chicago, IL, USA

facial nerve can be delineated on 9.4T MRI using DTI and the usefulness of this technique in the field of otopathology.

2 Materials and methods

Specimen preparation Whole temporal bone was removed from a deceased 1-year-old boy. The specimen was formalin-fixed, decalcified, and celloidin-embedded ex vivo and preserved in 80% ethanol [12].

Image acquisition MRI was performed on a Brucker 9.4 Tesla small animal scanner (Billerica, MA, USA) with an inner diameter of 11.6 cm and actively shielded gradient coils (maximum constant gradient strength for all axes: 230 mT/m). The specimen was placed within a Bruker 72 mm quad coil. The 3D T2-weighted fast spin-echo images were acquired using a rapid spin-echo sequence, with the following parameters: effective repetition time/echo time (TR/TE) = 4000 ms/20 ms; number of echoes = 8; number of averages = 4; matrix = 250 × 250; field of view = 50 mm; and voxel size = 0.2 × 0.2 × 0.2 mm. DTI was acquired in 30 directions, with the following parameters: matrix = 125 × 125; field of view = 50 mm; voxel size = 0.4 × 0.4 × 0.4 mm; TE = 19 ms; and *b* value = 3000. A total of 38 slices were scanned in a total scan time of approximately 15 h.

Image processing The imaging data were transferred to a workstation for DTI processing, including tensor estimation, acquisition of the color direction map, and co-registration with high-resolution T2-weighted images, using the BrainVoyager software, v20.6 (Brain Innovation, Maastricht, The Netherlands). The fractional anisotropy threshold was set at 0.15. Fiber tracking was not performed.

3 Results

The labyrinthine (Fig. 1), tympanic (Fig. 2), and mastoid (Fig. 3) segments of the facial nerve and the chorda tympani nerve (Fig. 4) were discernible on the color DTI and fractional anisotropy maps. The color directions of the facial nerve segments on the anisotropy maps were consistent with the orientation of the nerve bundles, changing appropriately with the curvature of the nerve (Fig. 5). However, no predominant directionality was evident in the geniculate ganglion, likely because of the presence of crisscrossing fibers. The osseous structures were readily visible with low signal intensity on the T2-weighted images, despite the decalcification of the specimen.

4 Discussion

This preliminary study showed that the intratemporal segments of the facial nerve could be delineated on DTI performed using 9.4 T MRI in vitro. The acquisition technique for isotropic resolution was essential to discern the small-caliber segments of the intratemporal facial nerve, including the chorda tympani. In particular, DTI could reliably depict the directionality of the nerve fibers, indicating that the nerve fibers remained intact in the specimen preservation process. Therefore, this approach could provide a complete multiplanar record for analyzing specimens that are subsequently sectioned for histological examination.

Although other MRI sequences, such as the pointwise encoding time reduction with radial acquisition and ultrashort echo time sequences, enable the visualization of the

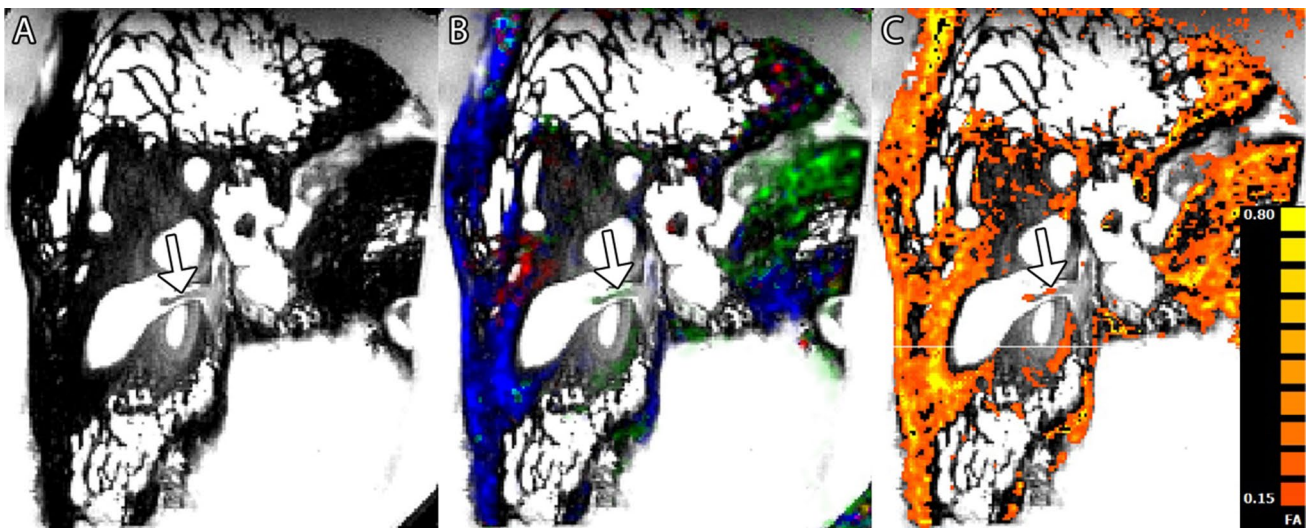

Fig. 1 T2-weighted magnetic resonance imaging (**a**), color diffusion tensor imaging (**b**), and fractional anisotropy map (**c**) demonstrate the length of the labyrinthine segment of the facial nerve (arrow)

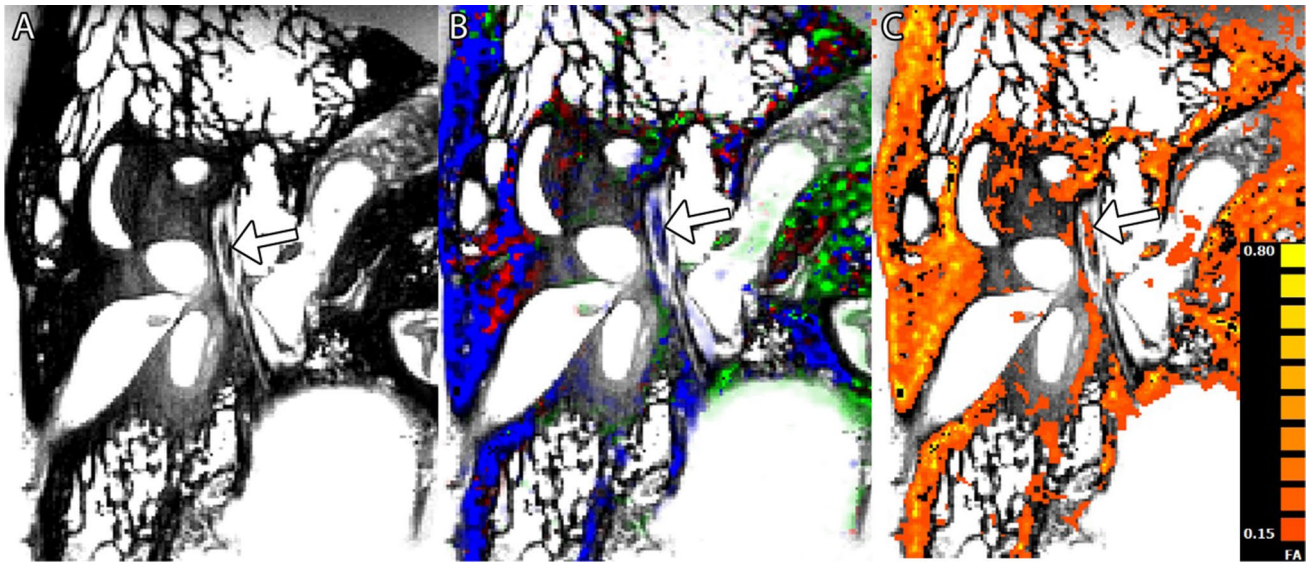

Fig. 2 T2-weighted magnetic resonance imaging (**a**), color diffusion tensor imaging (**b**), and fractional anisotropy map (**c**) demonstrate the length of the tympanic segment of the facial nerve (arrow)

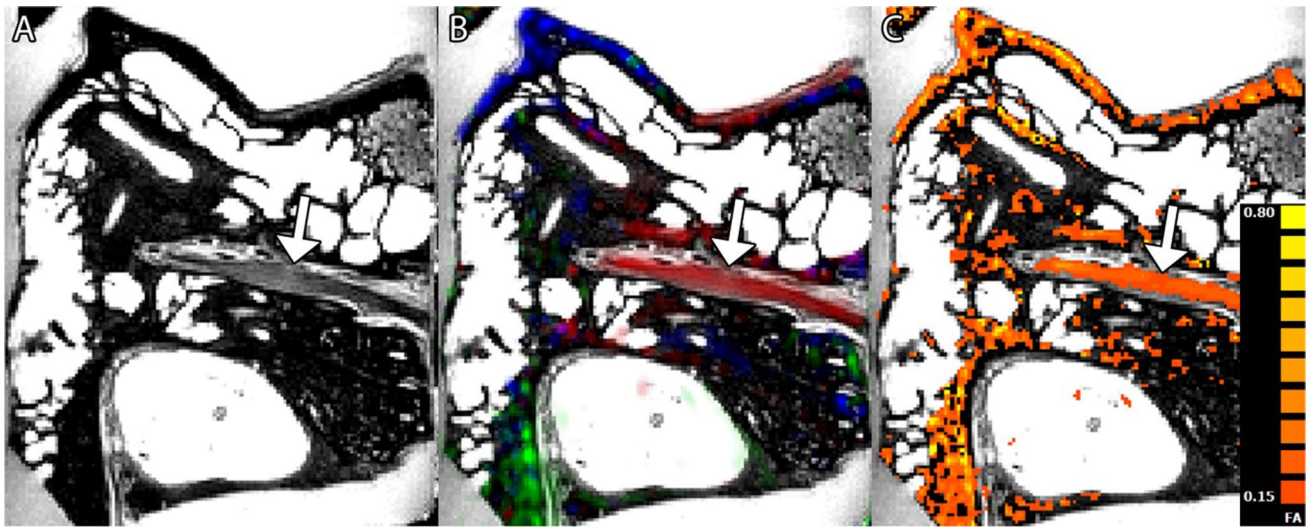

Fig. 3 T2-weighted magnetic resonance imaging (**a**), color diffusion tensor imaging (**b**), and fractional anisotropy map (**c**) demonstrate the length of the mastoid segment of the facial nerve (arrow)

facial nerve through the temporal bone without using intravenous contrast in vivo [13], DTI might offer additional data on the integrity of the facial nerve. For example, the degree of anisotropy could be predictive of the functional status in pathological cases that are planned for treatment. DTI might also be useful in establishing a more precise differential diagnosis, such as elucidating whether temporal bone tumors are intrinsic or extrinsic to the facial nerve, assessing post-traumatic lesions, and evaluating inflammatory processes such as Bell's palsy.

The technique described in this study might not directly be applicable to clinical scans, perhaps because of decalcification, fluid-filling of air-filled structures, and long scan times. For example, a high *b* value was used for DTI in this study to emphasize on the effect of restricted diffusion and to augment images using contrast, although a *b* value of 1000 has been effectively used to depict the facial nerve in the cerebellopontine cistern region for clinical applications [6, 14]. In addition, further investigations may be useful to assess the potential of DTI of the facial nerve using high-field clinical

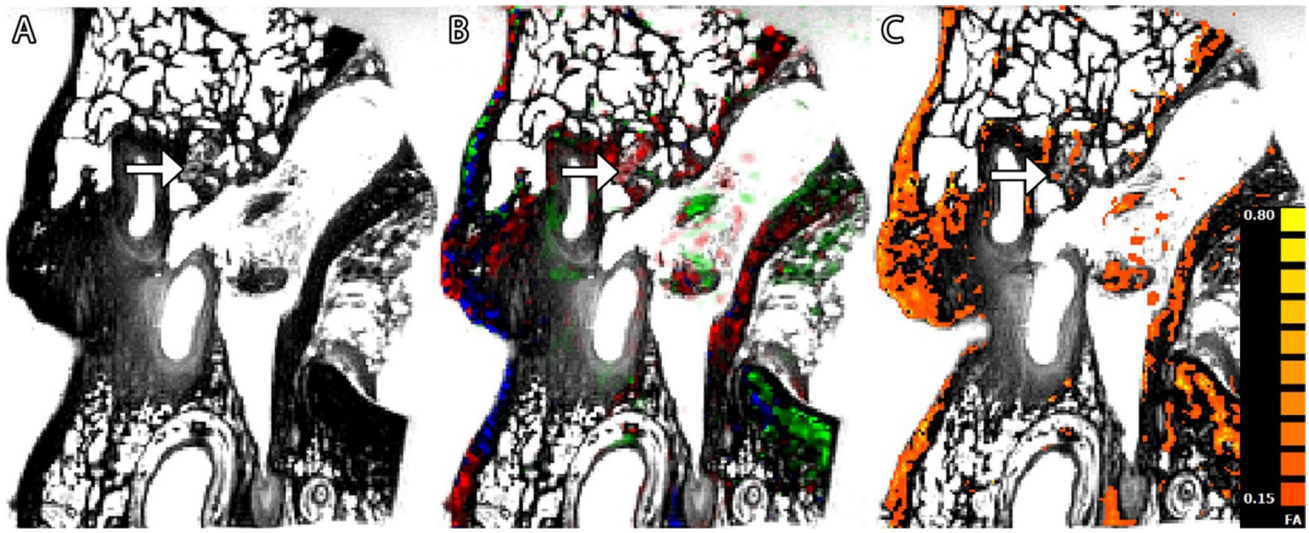

Fig. 4 T2-weighted magnetic resonance imaging (**a**), color diffusion tensor imaging (**b**), and fractional anisotropy map (**c**) demonstrate a cross section of the chorda tympani nerve (arrow)

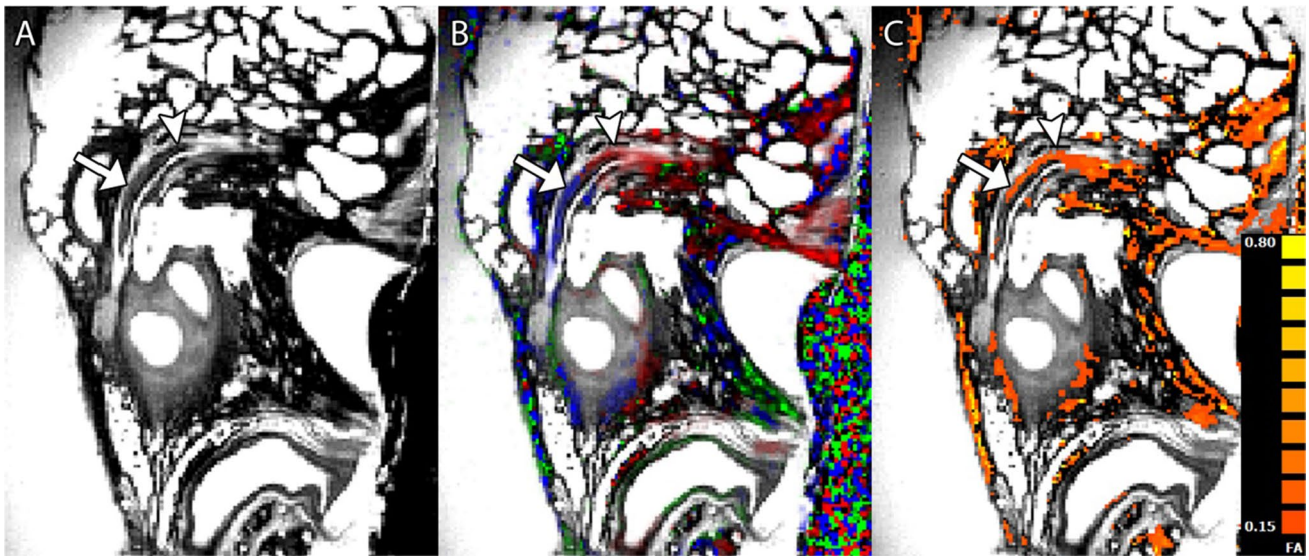

Fig. 5 T2-weighted magnetic resonance imaging (**a**), color diffusion tensor imaging (**b**), and fractional anisotropy map (**c**) demonstrate the second genu of the facial nerve with appropriate color changes from the tympanic segment (arrow) to the proximal mastoid segment (arrowhead)

scanners, such as 7 T MRI scanners, which have successfully been used to depict the inner ear structures in vivo [15].

With respect to the potential utility in the scheme of processing and examining temporal bone specimens in an otopathology lab, this technique might be useful as an additional means to archive anatomic features in rare specimens. The middle ear and mastoid air cells of the specimens are filled with celloidin, and the soft tissues in the specimen are saturated with 80% ethanol, which mitigates the inhomogeneity due to the presence of the air in these cavities. The main limitation of this study is that it is not directly applicable to in vivo measurements, as only cadaveric temporal bones were evaluated and only the T2-weighted sequence was used for imaging.

5 Conclusion

DTI performed using a high *b* value on 9.4 T MRI could help evaluate the intratemporal facial nerve in whole ex vivo specimens.

Funding This study was funded by the National Center for Advancing Translational Sciences of the National Institutes of Health through Grant Number UL1 TR000430.

Compliance with ethical standards

Conflict of interest The authors have no conflicts of interest or disclosures.

Ethical approval This article does not contain any studies with human participants or animals performed by any of the authors.

References

1. Lane JI, Witte RJ, Driscoll CL, Camp JJ, Robb RA. Imaging microscopy of the middle and inner ear: part I: CT microscopy. Clin Anat. 2004;17:607–12.
2. Lane JI, Witte RJ, Henson OW, Driscoll CL, Camp J, Robb RA. Imaging microscopy of the middle and inner ear: part II: MR microscopy. Clin Anat. 2005;18:409–15.
3. Thylur DS, Jacobs RE, Go JL, Toga AW, Niparko JK. Ultra-high-field magnetic resonance imaging of the human inner ear at 11.7Tesla. Otol Neurotol. 2017;38:133–8.
4. Kozerska M, Skrzat J. Anatomy of the fundus of the internal acoustic meatus—micro-computed tomography study. Folia Morphol (Warsz). 2015;74:352–8.
5. Li Z, Shi D, Li H, Tan S, Liu Y, Qi C, Tang A. Micro-CT study of the human cochlear aqueduct. Surg Radiol Anat. 2018;40:713–20.
6. Taoka T, Hirabayashi H, Nakagawa H, Sakamoto M, Myochin K, Hirohashi S, Iwasaki S, Sakaki T, Kichikawa K. Displacement of the facial nerve course by vestibular schwannoma: preoperative visualization using diffusion tensor tractography. J Magn Reson Imaging. 2006;24:1005–10.
7. Hilly O, Chen JM, Birch J, Hwang E, Lin VY, Aviv RI, Symons SP. Diffusion tensor imaging tractography of the facial nerve in patients with cerebellopontine angle tumors. Otol Neurotol. 2016;37:388–93.
8. Zhang Y, Mao Z, Wei P, Jin Y, Ma L, Zhang J, Yu X. Preoperative prediction of location and shape of facial nerve in patients with large vestibular schwannomas using diffusion tensor imaging-based fiber tracking. World Neurosurg. 2017;99:70–8.
9. Ung N, Mathur M, Chung LK, Cremer N, Pelargos P, Frew A, Thill K, Mathur I, Voth B, Lim M, Yang I. A systematic analysis of the reliability of diffusion tensor imaging tractography for facial nerve imaging in patients with vestibular schwannoma. J Neurol Surg B Skull Base. 2016;77:314–8.
10. Savardekar AR, Patra DP, Thakur JD, Narayan V, Mohammed N, Bollam P, Nanda A. Preoperative diffusion tensor imaging-fiber tracking for facial nerve identification in vestibular schwannoma: a systematic review on its evolution and current status with a pooled data analysis of surgical concordance rates. Neurosurg Focus. 2018;44:E5.
11. Măru N, Cheiţă AC, Mogoantă CA, Prejoianu B. Intratemporal course of the facial nerve: morphological, topographic and morphometric features. Rom J Morphol Embryol. 2010;51:243–8.
12. Nelson EG, Hinojosa R. Presbycusis: a human temporal bone study of individuals with downward sloping audiometric patterns of hearing loss and review of the literature. Laryngoscope. 2006;116:1–12.
13. Guenette JP, Seethamraju RT, Jayender J, Corrales CE, Lee TC. MR imaging of the facial nerve through the temporal bone at 3T with a noncontrast ultrashort echo time sequence. AJNR Am J Neuroradiol. 2018;39:1903–6.
14. Gerganov VM, Giordano M, Samii M, Samii A. Diffusion tensor imaging-based fiber tracking for prediction of the position of the facial nerve in relation to large vestibular schwannomas. J Neurosurg. 2011;115:1087–93.
15. van Egmond SL, Visser F, Pameijer FA, Grolman W. Ex vivo and in vivo imaging of the inner ear at 7 Tesla MRI. Otol Neurotol. 2014;35:725–9.